# Photosensitive Surfactants with Various Hydrophobic Tail Lengths for the Photocontrol of Genomic DNA Conformation with Improved Efficiency

## Antoine Diguet,[a] Naresh Kumar Mani,[a] Marie Geoffroy,[a] Matthieu Sollogoub,[b] and Damien Baigl*[a]

**Abstract:** We report the synthesis and characterisation of photosensitive cationic surfactants with various hydrophobic tail lengths. These molecules, called AzoCx, are used as photosensitive nucleic acid binders (pNABs) and are applied to the photocontrol of DNA conformation. All these molecules induce DNA compaction in a photodependent way, originating in the photodependent polarity of their hydrophobic tails. We show that increasing hydrophobicity strongly enhances the compaction efficiencies of these molecules, but reduces the possibility of reversible photocontrol of a DNA conformation. Optimal performance was achieved with AzoC5, which allowed reversible control of DNA conformation with light at a concentration seven times smaller than previously reported.

**Keywords:** azo compounds · DNA · hydrophobic interactions · photocontrol · surfactants

## Introduction

Genomic DNAs are long molecules (up to centimetres in contour length) that are compacted in nature to fit within narrow spaces such as viral capsids or nuclei in eukaryotic cells. Moreover, it has been well established that the higher-order structures of DNA and chromatin are crucial for the regulation of gene expression.[1] Several strategies to control DNA conformation and compaction in vitro have therefore been developed.[2] Most of them are based either on neutralising DNA negative charge with oppositely charged compounds (e.g., polyamines,[3] surfactants,[4] polymers,[3d, 5] nanoparticles[6] and vesicles[7]) or on creating unfavourable contacts with the solvent (e.g., crowding agents such as polyethylene glycol (PEG),[8] precipitation in alcohol[9] and solvents with low dielectric constants[10]). In most cases, DNA compaction is achieved by addition of a compaction agent to the DNA solution, whereas unfolding is usually achieved either by dilution or by addition of a second molecular species (e.g., monovalent salts,[11] compounds of high dielectric constant,[3b] or anionic surfactants[12]).[13] For all these strategies, the DNA conformation thus strongly depends on the composition of the surrounding medium, and controlling DNA conformation in a dynamic way under conditions of constant chemical composition remains challenging. To overcome such limitations, and bearing in mind potential reversible control of gene expression systems, we have developed a method for light-based reversible control of the conformation of genomic DNA,[14] which can in turn trigger biochemical reactions involved in gene expression.[15] In this approach, photocontrol of DNA conformation is achieved by addition to the DNA solution of a photosensitive nucleic acid binder (pNAB) molecule, the affinity of which for DNA can be modulated with light.[15] Only two pNABs have so far been reported. The first, usually referred to as AzoTAB, is a cationic surfactant containing an azobenzene group in its hydrophobic tail.[14,15] AzoTAB undergoes a *trans* to *cis* isomerisation at 365 nm accompanied by a change of polarity. The less polar *trans* isomer of AzoTAB can induce DNA compaction at a lower concentration than the more polar *cis* isomer. Consequently, there exists an AzoTAB concentration range for which genomic DNA is compacted under dark conditions but unfolded under UV illumination at 365 nm. AzoTAB has been successfully applied in the control of several photodependent properties involving DNA: control of the DNA conformation at the single-molecule level inside cell-mimicking microenviron-

[a] A. Diguet, N. K. Mani, M. Geoffroy, Prof. D. Baigl
Department of Chemistry, Ecole Normale Superieure
24 rue Lhomond, 75005 Paris (France)
Fax: (+33) 1-4432-2402
E-mail: damien.baigl@ens.fr

[b] Prof. M. Sollogoub
UPMC Univ Paris 06
Institut Parisien de Chimie Moléculaire (UMR CNRS 7201)
FR 2769, C. 181, 4 Place Jussieu, 75005 Paris (France)

Supporting information for this article is available on the WWW under http://dx.doi.org/10.1002/chem.201001579.

ments,[14b] release of DNA into cells[16] and photocontrol of gene expression systems both at transcription and at translation levels.[15] The photodependent polarity of this amphiphilic molecule has also been applied to develop photocontrollable surface tension properties and allowed us to manipulate droplets by using light.[17] The second type of pNAB is a photosensitive cationic gemini surfactant, referred to as AzoGEM, in which the *trans* to *cis* isomerisation is accompanied by changes both in polarity and in distance between cationic charges. Again, the *trans* isomer is more efficient than the *cis* isomer for induction of DNA compaction.

AzoTAB and AzoGEM show different capabilities for compaction of DNA as a function of light illumination. However, two important parameters have to be taken into account to evaluate the efficiency of a pNAB. The first is the concentration necessary to induce DNA compaction. Depending on buffer conditions, a 7000 to 20000 AzoTAB/ DNA molar ratio is necessary to achieve a photoreversible compaction.[14,15] This can be explained by the presence of only one cationic charge and the low hydrophobicities of both *trans* and *cis* isomers. Such a large excess of AzoTAB might be a drawback for some applications, especially in the context of in vivo implementations. In contrast, AzoGEM, which contains two cationic charges and two long hydrophobic tails, can induce DNA compaction at an AzoGEM/DNA molar ratio as low as 1.5.[18]

The other crucial parameter for assessment of pNAB efficiency is the reversibility of the DNA folding transition upon illumination: that is, the potential to induce DNA unfolding by illumination of a solution containing DNA molecules already compacted by the pNAB. AzoGEM can induce DNA compaction at a concentration corresponding to a 1.5-fold excess relative to DNA, but once the DNA has been compacted it cannot be unfolded regardless of illumination conditions.[18]

There is therefore a need to develop new pNAB molecules that can allow reversible photocontrol of DNA conformations at low concentrations. To this end, we synthesised a series of photosensitive cationic surfactants (AzoC$x$) homologous to AzoTAB but with various hydrophobic tail lengths (Figure 1 A). We studied the interaction of these molecules with genomic DNA in terms of their photodependent DNA compaction properties and the reversibility of the DNA folding transition.

## Results

Figure 1 A shows the molecular structures of the AzoC$x$ series. AzoC2 thus corresponds to the AzoTAB molecule described in other articles.[14,15,17] The compounds AzoC$x$ were prepared in three-step syntheses adapted from Hayashita et al.[19] Figure 1 B–D shows UV/Vis spectra of compounds AzoC$x$ in buffered solutions used for DNA compaction studies (10 mM TrisHCl, pH 7.5) as a function of time of illumination at 365 nm. All molecules show similar absorption spectra. In the absence of illumination the molecules
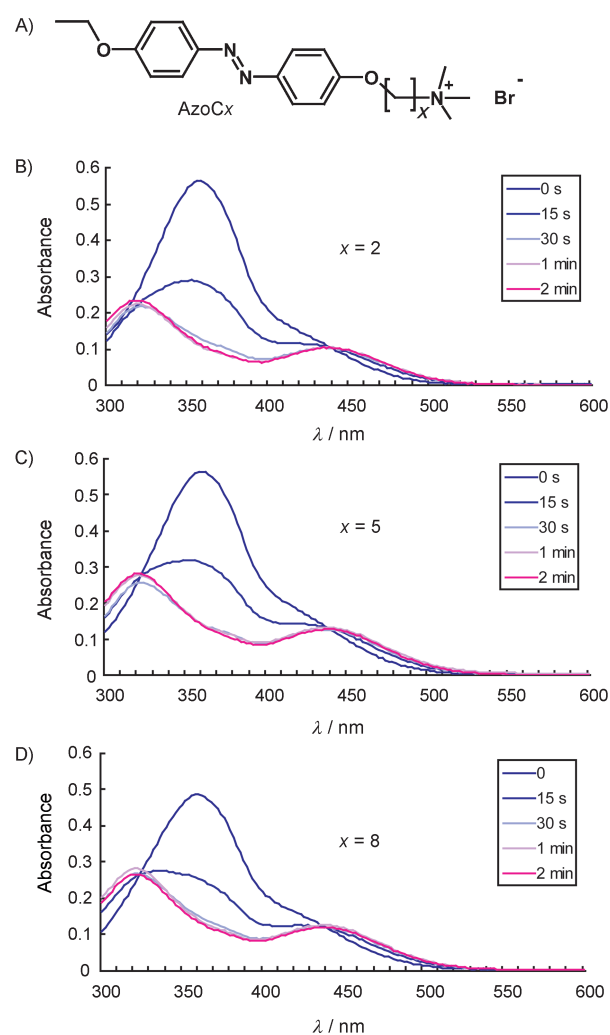


Figure 1. A) Molecular structures of the photosensitive surfactants AzoC$x$. B)–D) UV/Vis spectra of surfactants AzoC$x$ as a function of UV illumination time at 365 nm with $x=2$ (B), 5 (C) and 8 (D). Solutions were prepared in the buffer for DNA compaction studies (10 mM Tris·HCl, pH 7.5) at concentrations of 50 μM.

exist mainly in the *trans* configuration, which is characterised by a maximum at 360 nm. In the presence of UV light, the photostationary state contains a majority of *cis* isomer (maximum at 322 and 442 nm) and is typically reached after one minute of UV illumination regardless of the value of $x$.

To study the effect of hydrophobic tail length and of UV illumination on the hydrophobic character and auto-associative properties of the AzoC$x$ compounds, we determined their critical micellar concentrations (CMCs) by conductivity measurements with and without UV illumination at 365 nm. Each CMC was determined at the concentration at which a transition between two linear behaviour types was detected (Figure 2 for $x=2$ and Figure S1 in the Supporting Information for $x=5$ and $x=8$). Table 1 shows the CMC values obtained by these measurements. It shows that the CMCs, regardless of light illumination conditions, strongly decrease with increasing $x$, which is interpreted in terms of a
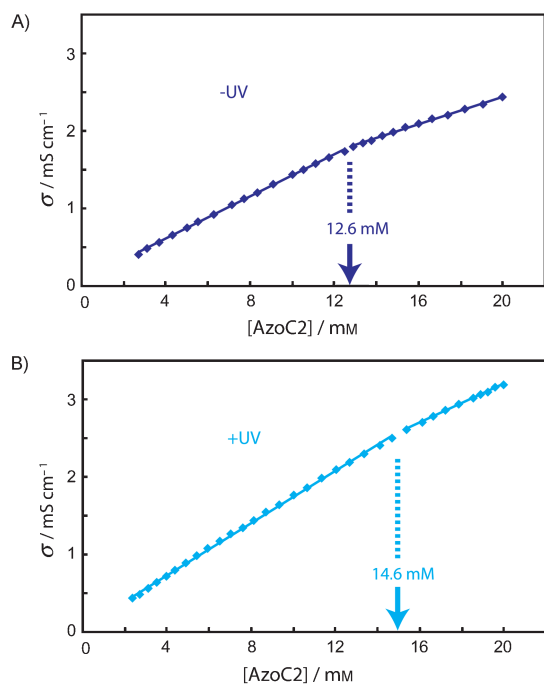
Figure 2. Conductivity ($\sigma$) as a function of AzoC2 concentration A) in the dark, and B) after UV illumination at 365 nm. Symbols are data points. Solid lines are linear fits. CMC is estimated at the concentration at which a transition between two linear behaviour types is observed (dashed line and arrow).



Figure 3. Typical fluorescence microscopy images of individual T4 DNA molecules (0.1 μM in 10 mM Tris·HCl buffer) in the presence of AzoC$x$ species at various concentrations, with (+UV) or without (−UV) illumination at 365 nm for 10 min prior to DNA addition to the solution. $T =$ 25 °C.

Table 1. Critical micellar concentrations (CMCs) for AzoC$x$ before (−UV) and after (+UV) illumination at 365 nm. Measurements were performed at (22±1) °C.

| Surfactant | AzoC2 | AzoC5 | AzoC8 |
|---|---|---|---|
| CMC [mM] −UV | 12.6 ± 0.2 | 0.83 ± 0.02 | 0.57 ± 0.02 |
| CMC [mM] +UV | 14.6 ± 0.3 | 0.90 ± 0.02 | 0.62 ± 0.02 |

higher propensity to self-assemble when the hydrophobic character of the tail is increased upon addition of methylene groups. Table 1 also shows that CMCs of the AzoC$x$ molecules are sensitive to illumination conditions. The CMCs are larger after UV illumination, regardless of $x$, which can be interpreted in terms of the more polar configuration of the *cis* isomer (after UV) compared with the *trans* isomer (visible/dark conditions). When CMC measurements were performed under the same conditions on a standard, non-photosensitive cationic surfactant, we did not detect any effect of UV illumination. For cetyltrimethylammonium bromide (CTAB), for instance, we measured a CMC of (0.95± 0.05) mM both before and after UV illumination. This control experiment supports the view that the effect of UV illumination on the CMCs of compounds AzoC$x$ is mainly due to the polarity changes resulting from the photoisomerisation of their azobenzene moieties.

We characterised the conformations of a large number of individual genomic DNA molecules (T4 DNA, 166 kbp) by fluorescence microscopy observations of very dilute solutions (Figure 3). In the absence of AzoC$x$, all DNA mole-
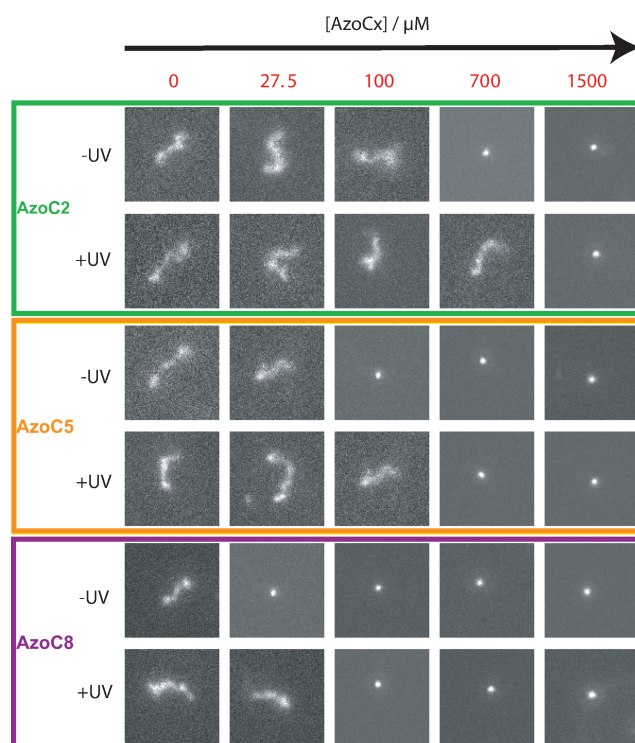
cules show elongated coil conformations, due to the electrostatic repulsions between charged phosphate groups along the DNA chain, and typical intrachain fluctuations, which are the signature of an unfolded state. In contrast, in the presence of a sufficiently high concentration of an AzoC$x$ species, all DNA molecules appear as bright, fast-diffusing spots corresponding to compact DNA states. Figure 3 shows that for a given DNA concentration (here 0.1 μM) the characteristic AzoC$x$ concentrations corresponding to the transition between the unfolded and the compact state strongly depend on $x$ and on the illumination conditions. Regardless of illumination conditions, DNA compaction occurs at smaller AzoC$x$ concentrations with increasing $x$. Conversely, regardless of $x$, UV illumination is accompanied by increases in the AzoC$x$ concentrations required to compact the DNA, indicating lower compaction efficiencies of the *cis*-AzoC$x$ isomers than their *trans* counterparts.

To quantify these observations, we established the DNA compaction curves, that is, the proportion of DNA molecules in the compact state as a function of AzoC$x$ concentration. Figure 4 shows the compaction curves with and without illumination at 365 nm for 10 min before DNA addition. The curves shown in Figure 4 are consistent with the qualitative observations shown in Figure 3. Without UV illumination (*trans*-AzoC$x$), the minimum AzoC$x$ concentrations [AzoC$x$]* for which 100% of DNA molecules are in the
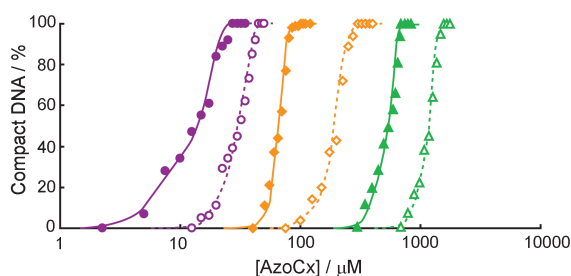
Figure 4. Lin-log plots of the percentages of T4 DNA molecules in the compact state as a function of AzoC*x* concentration with (open symbols) or without (filled symbols) illumination at 365 nm for 10 min prior to DNA introduction. Symbols are data points. Solid and dashed lines are guidelines for the eyes for −UV and +UV conditions, respectively. [T4 DNA]=0.1 μM in 10 mM Tris·HCl buffer. $T=25\,°C$. ▲=AzoC2 −UV, △=AzoC2 +UV, ◆=AzoC5 −UV, ◇=AzoC5 +UV, ●=AzoC8 −UV, ○=AzoC8 +UV.

compact state decrease with increasing *x* ([AzoC*x*]*=700, 100 and 27.5 μM for *x*=2, 5 and 8, respectively). When the AzoC*x* samples had been illuminated under UV before DNA addition (*cis*-AzoC*x*), the same trend was observed but the AzoC*x* concentrations required for full DNA compaction were significantly higher ([AzoC*x*]*=1500, 300 and 45 μM for *x*=2, 5 and 8, respectively). All these results show that both the *cis*- and the *trans*-AzoC*x* isomers have stronger DNA compaction efficiencies when the lengths of the hydrophobic tails are greater and that, regardless of *x*, the *cis* isomers are less efficient than the *trans* isomers in inducing DNA compaction. Again, when the same experiment was performed with a non-photosensitive cationic surfactant (CTAB), we did not observe any effect of UV illumination on the compaction curves (Figure S2 in the Supporting Information), indicating that the photodependence of the DNA compaction efficiency is due to the photoisomerisation of the AzoC*x* hydrophobic tails. Finally, it is interesting to note that for each AzoC*x* molecule there is a range of [AzoC*x*] in which the proportion of DNA molecules in the compact state dramatically depends on UV illumination conditions. Table 2 shows some characteristic [AzoC*x*]

Table 2. Percentages of DNA molecules in the compact state with (+UV) or without (−UV) illumination at 365 nm for 10 min prior to DNA addition to the solution at the minimum AzoC*x* concentration needed to achieve full compaction in the absence of UV. $T=25\,°C$.

| Surfactant | AzoC2 (700 μM) | AzoC5 (100 μM) | AzoC8 (27.5 μM) |
|---|---|---|---|
| compact DNA [%] −UV | 100 | 100 | 100 |
| compact DNA [%] +UV | 0 | 4 | 39 |

values at which most DNA molecules are in the compact state and in the unfolded state in the absence and in the presence of UV illumination, respectively.

A crucial parameter for photocontrollable DNA compaction systems is the reversibility of DNA conformational transitions upon illumination. To assess the photoreversibili-

ty of the DNA/AzoC*x* systems, we first added the AzoC*x* to the DNA solution to provide 95% of DNA molecules in the compact state. We then applied illumination at 365 nm and characterised the conformational state of a large number of individual DNA molecules by fluorescence microscopy. Figure 5 shows the proportions of DNA molecules in the
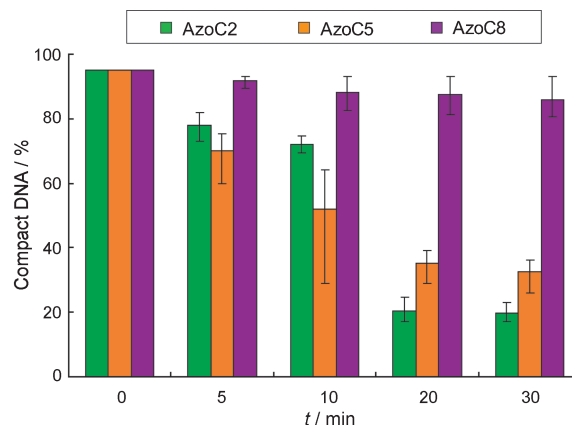


Figure 5. Percentages of DNA molecules in the compact state after illumination of DNA solutions at 365 nm for a time *t*. The AzoC*x* concentrations were chosen to provide 95% of compact state at $t=0$. [AzoC*x*]=690, 80 and 18.5 μM for *x*=2, 5 and 8, respectively. Colour bars and error bars show average and min/max values for three replicates. [T4 DNA]=0.1 μM in 10 mM Tris·HCl buffer. $T=25\,°C$.

compact state as a function of the UV illumination time (*t*). For AzoC2 and AzoC5 it shows that most of the DNA molecules have unfolded after 20 min of UV illumination, with only about 20 and 35% of molecules, respectively, remaining in the compact state. This demonstrates the potential to unfold compact DNA by use of light both for DNA/AzoC2 and for DNA/AzoC5 systems. In the presence of AzoC8, in contrast, most DNA molecules remain in the compact state regardless of UV illumination time. After 30 min of UV illumination about 85% of molecules remain in the compact state. These results show that the lengths of the hydrophobic chains of AzoC*x* have a dramatic influence on the photoreversible control of DNA conformation.

Figure 5 shows that the proportions of compact DNA decrease with increasing UV illumination time. To describe the process of DNA unfolding upon UV illumination more precisely, we measured the apparent long-axis lengths ($L_{DNA}$) of a large number of individual DNA molecules before and after illumination at 365 nm for 20 min. Figure 6 shows the resulting DNA size distributions in the absence of AzoC*x* (Figure 6 A) and in the presence of AzoC*x* concentrations corresponding to 95% in the compact state before illumination ([AzoC*x*]=690, 80 and 18.5 μM for *x*=2, 5 and 8, respectively). In the absence of AzoC*x*, the $L_{DNA}$ value is around 3.5 μm, both before and after UV illumination, which confirms that UV exposure has no significant effect on DNA chain integrity under these illumination conditions. In the presence of AzoC*x*, most DNA molecules are in the
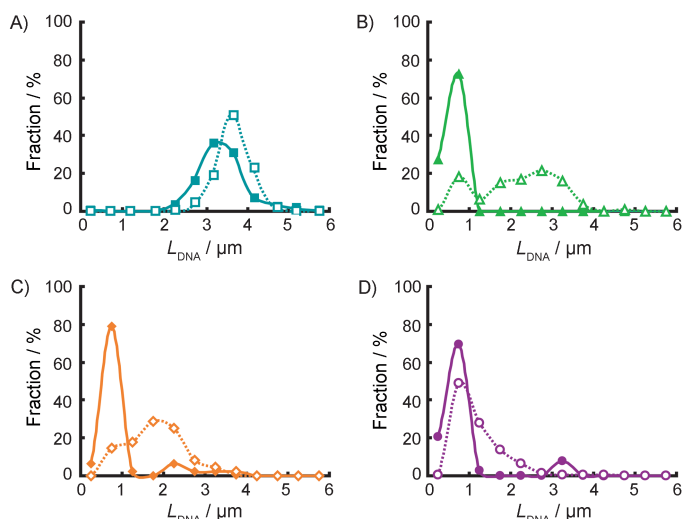
Figure 6. A)–D) Distribution of DNA long-axis lengths ($L_{DNA}$): A) in the absence of AzoC$x$, and in the presence of B) [AzoC2] = 690 μM, C) [AzoC5] = 80 μM, and D) [AzoC8] = 18.5 μM, before (−UV, filled symbols) and after (+UV, open symbols) illumination of the DNA solutions at 365 nm for 20 min. Symbols represent the percentages of DNA molecules of size $L_{DNA}$ ± 0.25 μm. Solid and dashed lines are guidelines for the eyes for −UV and +UV conditions, respectively. [T4 DNA] = 0.1 μM in 10 mM Tris·HCl buffer. $T$ = 25 °C.

compact state and show narrow distributions centred on 0.75 μm regardless of $x$. Such distributions are very similar to those obtained when DNA is compacted by a conventional condensing agent such as spermine.[3] By fluorescence microscopy, these DNA condensates, which are around 100 nm in size, appear as bright moving spots with apparent long-axis lengths between 0.5 and 1 μm due to the blurring effect of fluorescence.[20] For all AzoC$x$ molecules, UV illumination results in the appearance of DNA molecules of larger size (between 1 and 4 μm), which indicates a process of partial to complete unfolding, but the extent of this unfolding strongly depends on $x$. Firstly, the proportion of molecules remaining in a compact state ($L_{DNA} \leq 1.25$ μm) increases with increasing $x$, consistently with Figure 5. Secondly, the lengths of unfolded molecules ($L_{DNA} > 1.25$ μm) also depend on $x$. The maximum of the distribution, for instance, decreases with increasing $x$ (2.75, 1.75 and 0.75 μm for $x$ = 2, 5 and 8, respectively). According to fluorescence microscopy observations, for AzoC2 and AzoC5, unfolded DNA molecules after UV illumination have an elongated coil shape very similar to that of naked DNA in the absence of AzoC$x$ (with or without UV illumination) but their sizes tend to be smaller on average. In the case of AzoC8, only a few DNA molecules show an elongated coil conformation and they coexist with swollen globules. All these results show that UV illumination of DNA initially compacted by AzoC$x$ induces partial to complete DNA unfolding with characteristics that strongly depend on the hydrophobic chain length of the AzoC$x$ species.

## Discussion

AzoC$x$ molecules are cationic surfactants containing photo-isomerisable azobenzene group in their hydrophobic tails. Regardless of $x$, the *cis* isomers are more polar and therefore less prone to self-assemble than the *trans* isomers. This is confirmed by the CMC values of the AzoC$x$ species, which are systematically larger after UV illumination (*cis* isomers) than in the absence of UV (*trans* isomers) regardless of $x$ (Table 1). Like CTAB or other cationic surfactants,[4] AzoC$x$ compounds can interact electrostatically with DNA and induce DNA compaction at sufficiently high AzoC$x$ concentrations. Moreover, it has been well established from the pioneering works of Hayakawa et al. that the binding of cationic surfactants to DNA is highly cooperative.[21] We thus suggest that, regardless of $x$, the *cis*-AzoC$x$ compounds, which are less able to form aggregates than the *trans*-AzoC$x$ compounds, are less efficient in cooperatively binding to DNA and therefore induce DNA compaction at higher concentrations than *trans*-AzoC$x$ compounds, which can cooperatively bind to DNA in a more efficient way. As a consequence, full DNA compaction is achieved at smaller AzoC$x$ concentrations in the absence of UV (*trans* isomers) than after UV illumination (*cis* isomers) prior to DNA introduction (Figure 3 and Figure 4 and Table 2).

In the AzoC$x$ series, the lengths and hydrophobicities of the AzoC$x$ tails increase with increasing $x$ for both *trans* and *cis* isomers. This explains why the CMCs of compounds AzoC$x$ significantly decrease with increasing $x$ both for −UV (*trans* isomers) and for +UV (*cis* isomers) conditions (Table 1). Therefore, for a given *trans* or *cis* isomer, an increase in $x$ enhances the potential of AzoC$x$ to self-assemble, thus promoting its cooperative binding to DNA. As a consequence, both for −UV and for +UV illumination conditions, the AzoC$x$ concentrations necessary to achieve full DNA compaction strongly decrease with increasing $x$ (Figure 3, Figure 4 and Table 2). This concentration decreases 25 times, for instance, when $x$ increases from 2 to 8. This enhancement of DNA compaction with increasing hydrophobicity is not specific to AzoC$x$ molecules. It has also been reported in the case of non-photosensitive cationic surfactants[22] as well as with gemini surfactants.[18]

We saw that the photodependence of the polarities of AzoC$x$ species induces marked DNA compaction efficiency differences between their *trans* (−UV, stronger compaction agents) and *cis* (+UV, weaker compaction agents) isomers and that the DNA compaction efficiencies of both *trans*- and *cis*-AzoC$x$ can be strongly enhanced with increasing $x$. One should thus consider the potential to switch DNA from a compact state to an unfolded state on application of UV light to DNA initially compacted by different AzoC$x$ molecules. We found that DNA compacted by AzoC2 or AzoC5 can be efficiently (yet not totally) unfolded upon UV illumination, whereas DNA compacted by AzoC8 mainly remains in a compact or very partially unfolded state even after a long UV exposure time (Figure 5 and Figure 6). Two interpretations can be proposed to explain the difference be-

tween AzoC8 and the other AzoC$x$ compounds ($x = 2$ and 5). Firstly, as shown in Figure 4 and Table 1, the differences in the compaction efficiencies of the *trans* and *cis* isomers are more pronounced for AzoC2 and AzoC5 than for AzoC8, probably as a result of the decrease in the efficiency of azobenzene isomerisation in inducing a polarity change when additional methylene groups are inserted in the hydrophobic tail. This trend is confirmed by the effect of UV illumination on the CMC values, which decreases with increasing $x$ (Table 1). Secondly, compact DNA molecules that have been unfolded by exposure to UV are significantly less elongated in the case of DNA/AzoC8 than in those of the DNA/AzoC5 and DNA/AzoC2 systems (Figure 6). This is probably due to the increase in hydrophobic interactions with increasing $x$, which might stabilise compact conformations of DNA/AzoC$x$ complexes. All these results show that, in the AzoC$x$ series, increasing hydrophobicity corresponds to a better DNA compaction efficiency, but reduces the potential for reversible control over the conformation of DNA with the aid of light.

## Conclusion

We have described for the first time the synthesis and characterisation of photosensitive surfactants (AzoC$x$ compounds) with various hydrophobic tail lengths for photocontrol over genomic DNA conformations. For all AzoC$x$ molecules, the *trans* isomers are more efficient in DNA compaction than their *cis* counterparts. We found that increasing hydrophobicity greatly enhances the ability of AzoC$x$ to compact DNA, but limits the potential for reversible control over DNA conformation through the use of light. These results were interpreted in terms of cooperative interaction between the AzoC$x$ species and DNA, and the role of hydrophobic interactions in the stabilisation of the compact conformations of DNA/AzoC$x$ systems had been proposed. AzoC5 represents a good compromise between compaction efficiency and photoreversibility. It is seven times more efficient than AzoC2 in compacting DNA and, unlike AzoC8, it can be used for the reversible photocontrol of DNA conformation.

To develop more efficient photosensitive nucleic acid binders (pNABs) we are now exploring other strategies based on the use of multivalent cationic molecules with polarities or valencies that can be reversibly modulated through the action of light, which should allow reversible photocontrol of DNA conformations at very low pNAB/DNA charge ratios. Finally, in view of the considerable range of applications of photosensitive surfactants in the photocontrol of physicochemical and biological phenomena,[23,24] such as gene expression,[15] protein folding,[25] gene delivery,[16] sol/gel transition,[26] or droplet manipulation,[17] this work is a contribution to the rational development of efficient smart photoresponsive systems.

## Experimental Section

**Materials**: Bacteriophage T4 DNA (166 kb) was from Wako Chemicals. YOYO-1 iodide was from Molecular Probes. All other chemicals were purchased from Sigma. Deionised water (Millipore, 18 MΩ cm$^{-1}$) was used for all experiments.

**Synthesis**: AzoC2 was synthesised by the method described by Hayashita et al.[19] Other AzoC$x$ molecules were prepared analogously, by azocoupling of *p*-ethoxyaniline with phenol, followed by alkylation and quaternisation with dibromoalkane and trimethylamine, respectively.

**Synthesis of AzoH**: Concentrated HCl (17 mL) and ice (80 g) were added to an ethanol/water solution (1:1, 160 mL) containing *p*-ethoxyaniline (10.4 mL, 80 mmol) and sodium nitrite (5.5 g, 80 mmol) in an ice bath. Cold water (42 mL) containing phenol (7.5 g, 80 mmol) and NaOH (6.4 g, 160 mmol) was then carefully added to the solution, and the mixture was stirred for 90 min. The pH of the solution was adjusted to 1.0 with HCl and it was left to stand for 30 min. The resulting precipitate was filtered, washed with pure water and dried under vacuum. Yield: 92% (brown powder); $^1$H NMR (250 MHz, CDCl$_3$): $\delta = 7.89$ (d, $^3J$-(H,H) = 9.0 Hz, 2H; Ar-H), 7.84 (d, $^3J$(H,H) = 8.7 Hz, 2H; Ar-H), 7.01 (d, $^3J$ = 8.9 Hz, 2H; Ar-H), 6.95 (d, $^3J$ = 8.6 Hz, 2H; Ar-H), 4.13 (q, $^3J$-(H,H) = 7.0 Hz, 2H; CH$_2$), 1.48 ppm (t, $^3J$(H,H) = 7.0 Hz, 3H; CH$_3$); $^{13}$C NMR (250 MHz, CDCl$_3$): $\delta = 161.1$ (Ar-C), 158.2 (Ar-C), 147.0 (Ar-C), 146.8 (Ar-C), 124.6 (Ar-C), 124.4 (Ar-C), 115.9 (Ar-C), 114.8 (Ar-C), 63.9 (CH$_2$), 14.8 ppm (CH$_3$); MS (CI): $m/z$: calcd for C$_{14}$H$_{14}$N$_2$O$_2$: 242.3 [$M$]$^+$; found: 242.1.

**Synthesis of Azo5Br**: The azobenzene precursor AzoH (610 mg, 2.5 mmol) was dissolved in anhydrous ethanol (12.5 mL) containing NaOH (100 mg, 3.0 mmol) and the mixture was stirred for 30 min. Anhydrous ethanol (5.4 mL) containing 1,5-dibromopentane (1.0 mL, 7.5 mmol) was slowly added (10 min) and the mixture was heated at reflux for two days. The solvent was evaporated under vacuum. The remaining solid was dissolved in dichloromethane (10 mL) and extractions were performed with NaOH solution (1 M, 2×4 mL) and pure water (2× 4 mL). The organic phase was dried with MgSO$_4$ and concentrated. Yield: 62% (orange powder); $^1$H NMR (250 MHz, CDCl$_3$): $\delta = 7.92$ (q, $^3J$(H,H) = 8.9 Hz, 4H; Ar-H), 7.02 (d, $^3J$(H,H) = 8.8 Hz, 4H; Ar-H), 4.16 (q, $^3J$(H,H) = 7.0 Hz, 2H; CH$_2$O), 4.11 (t, $^3J$(H,H) = 6.3 Hz, 2H; CH$_2$O), 3.50 (t, $^3J$(H,H) = 6.7 Hz, 2H; CH$_2$Br), 2.06–1.90 (m, 2H; CH$_2$), 1.95–1.82 (m, 2H; CH$_2$), 1.70–1.60 (m, 2H; CH$_2$), 1.50 ppm (t, $^3J$(H,H) = 6.9 Hz, 3H; CH$_3$); $^{13}$C NMR (250 MHz, CDCl$_3$): $\delta = 161.0$ (Ar-C), 147.0 (Ar-C), 124.4 (Ar-C), 114.7 (Ar-C), 67.9 (CH$_2$O), 63.8 (CH$_2$O), 33.5 (CH$_2$), 32.5 (CH$_2$), 28.4 (CH$_2$Br), 24.8 (CH$_2$), 14.8 ppm (CH$_3$); MS (IC): $m/z$: calcd for C$_{19}$H$_{23}$N$_2$O$_2$Br: 391.3 [$M$]$^+$; found: 390.2.

**Synthesis of AzoC5**: The dried Azo5Br product (605 mg, 0.87 mmol) was dissolved in dry THF (50 mL), trimethylamine gas was bubbled through the solution for 30 min, and the solution was left for six days. The resulting precipitate was filtered, washed with THF, and dried under vacuum. The product was recrystallised twice from ethanol. Yield: 53% (orange powder); $^1$H NMR (500 MHz, DMSO): $\delta = 7.84$ (d, $^3J$(H,H) = 6.6 Hz, 2H; Ar-H), 7.82 (d, $^3J$(H,H) = 6.6 Hz, 2H; Ar-H), 7.12 (d, $^3J$(H,H) = 6.7 Hz, 2H; Ar-H), 7.10 (d, $^3J$(H,H) = 6.7 Hz, 2H; Ar-H),), 4.10 (m, 2H; CH$_2$O), 3.99 (q, $^3J$(H,H) = 8.4 Hz, 2H; CH$_2$O), 3.39–3.34 (m, 2H; CH$_2$N), 3.06 (s, 9H; CH$_3$N), 1.85–1.71 (m, 4H; CH$_2$), 1.34–1.49 (m, 2H; CH$_2$), 1.34 ppm (t, $^3J$(H,H) = 6.8 Hz, 3H; CH$_3$); $^{13}$C NMR (250 MHz, DMSO): $\delta = 160.8$ (Ar-C), 146.0 (Ar-C), 124.1 (Ar-C), 114.9 (Ar-C), 67.5 (CH$_2$O), 65.2 (CH$_2$N), 63.6 (CH$_2$O), 52.2 (CH$_3$N), 28.0 (CH$_2$), 22.4 (CH$_2$), 21.8 (CH$_2$), 14.6 ppm (CH$_3$); MS (ESI): $m/z$: calcd for C$_{22}$H$_{32}$N$_3$O$_2$: 370.5 [$M - $Br$^-$]$^+$; found: 370.3.

**Synthesis of Azo8Br**: The azobenzene precursor AzoH (610 mg, 2.5 mmol) was dissolved in anhydrous ethanol (12.5 mL) containing NaOH (100 mg, 2.5 mmol) and the mixture was stirred for 30 min. 1,8-Dibromooctane (1.4 mL, 7.5 mmol) was slowly added (10 min) and the solution was heated at reflux for two days. The solvent was evaporated under vacuum. The remaining solid was dissolved in dichloromethane (10 mL) and extractions were performed with NaOH solution (1 M, 2×4 mL) and pure water (2×4 mL). The organic phase was dried with MgSO$_4$ and con-

centrated. Yield: 71% (orange powder); $^1$H NMR (250 MHz, CDCl$_3$): $\delta = 7.72$ (d, $^3J$(H,H) $= 8.9$ Hz, 4H; Ar-H), 6.92 (d, $^3J$(H,H) $= 8.9$ Hz, 4H; Ar-H), 4.10 (q, $^3J$(H,H) $= 7.0$ Hz, 2H; CH$_2$O), 3.98 (t, $^3J$(H,H) $= 6.6$ Hz, 2H; CH$_2$O), 3.35 (t, $^3J$(H,H) $= 6.7$ Hz, 2H; CH$_2$Br), 1.89–1.71 (m, 4H; CH$_2$), 1.42–1.22 ppm (m, 8H; CH$_2$+CH$_3$); $^{13}$C NMR (250 MHz, CDCl$_3$): $\delta = 160.8$ (Ar-C), 147.0 (Ar-C), 124.3 (Ar-C), 114.7 (Ar-C), 68.2 (CH$_2$O), 63.8 (CH$_2$O), 33.9 (CH$_2$), 32.0 (CH$_2$), 29.7 (CH$_2$Br), 29.2 (CH$_2$), 28.7 (CH$_2$), 28.1 (CH$_2$), 25.9 (CH$_2$), 14.8 ppm (CH$_3$); MS (IC): $m/z$: calcd for C$_{22}$H$_{29}$N$_2$O$_2$Br: 433.4 [$M$]$^+$; found: 432.2.

**Synthesis of AzoC8**: The dried Azo8Br product (766 mg, 1.77 mmol) was dissolved in dry THF (30 mL), trimethylamine gas was bubbled through the solution for 30 min, and the solution was left for two days. The resulting precipitate was filtered, washed with THF and dried under vacuum. The product was recrystallised from isopropanol. Yield: 46% (orange powder); $^1$H NMR (500 MHz, CDCl$_3$): $\delta = 7.80$ (d, $^3J$(H,H) $= 8.9$ Hz, 4H; Ar-H), 6.90 (d, $^3J$(H,H) $= 8.9$ Hz, 4H; Ar-H), 4.05 (q, $^3J$(H,H) $= 8.7$ Hz, 2H; CH$_2$O), 3.97 (t, $^3J$(H,H) $= 8.0$ Hz, 2H; CH$_2$O), 3.56–3.51 (m, 2H; CH$_2$N), 3.37 (s, 9H; CH$_3$N), 1.81–1.62 (m, 4H; CH$_2$), 1.43 (t, $^3J$(H,H) $= 8.7$ Hz, 3H; CH$_3$), 1.35–1.25 ppm (m, 8H; CH$_2$); $^{13}$C NMR (250 MHz, CDCl$_3$): $\delta = 161.1$ (Ar-C), 147.0 (Ar-C), 124.3 (Ar-C), 114.7 (Ar-C), 68.1 (CH$_2$O), 67.0 (CH$_2$N), 63.8 (CH$_2$O), 53.5 (CH$_3$N), 29.1 (CH$_2$+CH$_2$), 29.0 (CH$_2$), 26.1 (CH$_2$), 25.8 (CH$_2$), 23.2 (CH$_2$), 14.8 ppm (CH$_3$); MS (ESI): $m/z$: calcd for C$_{25}$H$_{38}$N$_3$O$_2$: 412.6 [$M-$Br]$^+$; found: 412.3.

**Preparation of DNA samples**: Water, Tris·HCl buffer, YOYO-1 iodide and photosensitive surfactant were mixed in this order prior to careful T4 DNA introduction under low-shear conditions to avoid DNA breakage.[11] For all experiments, we used T4 DNA at a final concentration of 0.1 μM (concentration in nucleotides) in Tris·HCl buffer (10 mM, pH 7.4) with YOYO (0.01 μM) as a DNA fluorescent dye. For all steps except UV illuminations, DNA samples were kept under dark conditions. Samples were equilibrated for 15 min prior to DNA characterisation by fluorescence microscopy.

**UV illumination**: For all experiments except CMC measurements, UV exposure was performed by placing the sample in a 1.5 mL tube (Eppendorf) at 6–8 cm distance from a UV lamp (Vilber Lourmat, 6 W) at 365 nm. For CMC measurements, the solution (5 mL) was placed in a 50 mL plastic tube at 6–8 cm distance from a UV lamp (45 W), working at 365 nm for 30 min.

**UV/Vis spectroscopy**: The solution (200 μL) was introduced into a well of a 96-well microplate and analysed by use of a Synergy HT microplate reader (Biotek Instruments) with Gen5 acquisition software. The reference background was determined by measurement of the spectrum of the same amount of pure water.

**Critical micellar concentration (CMC) measurements**: CMC determination was achieved by conductivity measurements of solutions with the aid of a C860 conductimeter (Consort). The sample was carefully homogenised and equilibrated at $(22\pm1)$ °C prior to measurement.

**Fluorescence microscopy**: Fluorescence microscopy was performed with an AxioObserver D1 inverted microscope (Zeiss), fitted with a 100 × oil-immersed objective lens. Images were acquired with a highly sensitive EM-CCD camera (Photonmax 512B, Princeton Scientific) and Metavue image acquisition software (Molecular Devices). DNA molecules were observed in 20 μL droplets deposited on a clean glass cover slide. For each set of conditions, a minimum of 200 individual DNA molecules were characterised to determine the fraction of molecules in the compact state (Figure 4 and 5). Each size distribution shown in Figure 6 was established by measuring the long-axis lengths (longest distance in the outline of DNA image) on 50 individual molecules in three replicates with the aid of ImageJ software.

## Acknowledgements

[1] a) S. B. Baylin, K. E. Schuebel, *Nature* **2007**, *448*, 548–549; b) A. Bird, *Nature* **2007**, *447*, 396–398; c) B. Li, M. Carey, J. L. Workman, *Cell* **2007**, *128*, 707–719; d) R. Métivier, *Nature* **2008**, *452*, 45–52; e) B. Dorigo, T. Schalch, A. Kylangara, S. Duda, R. R. Schroeder, T. J. Richmond, *Science* **2004**, *306*, 1571–1573; f) N. J. Francis, R. E. Kingston, C. L. Woodcock, *Science* **2004**, *306*, 1574–1577.

[2] V. A. Bloomfield, *Curr. Opin. Struct. Biol.* **1996**, *6*, 334–341; V. A. Bloomfield, *Biopolymers* **1997**, *44*, 269–282.

[3] a) L. C. Gosule, J. A. Schellman, *Nature* **1976**, *259*, 333–335; b) D. Baigl, K. Yoshikawa, *Biophys. J.* **2005**, *88*, 3486–3493; c) A. A. Zinchenko, K. Yoshikawa, D. Baigl, *Adv. Mater.* **2005**, *17*, 2820–2823; d) W.-H. Huang, A. A. Zinchenko, C. Pawlak, Y. Chen, D. Baigl, *ChemBioChem* **2007**, *8*, 1771–1774.

[4] S. M. Mel'nikov, V. G. Sergeyev, K. Yoshikawa, *J. Am. Chem. Soc.* **1995**, *117*, 2401–2408.

[5] a) U. K. Laemmli, *Proc. Natl. Acad. Sci. USA* **1975**, *72*, 4288–4292; b) R. S. Dias, A. A. C. C. Pais, M. G. Miguel, B. Lindman, *J. Chem. Phys.* **2003**, *119*, 8150–8157.

[6] a) A. A. Zinchenko, K. Yoshikawa, D. Baigl, *Phys. Rev. Lett.* **2005**, *95*, 228101; b) A. A. Zinchenko, T. Sakaue, S. Araki, K. Yoshikawa, D. Baigl, *J. Phys. Chem. B* **2007**, *111*, 3019–3031.

[7] A. Diguet, D. Baigl, *Langmuir* **2008**, *24*, 10604–10607.

[8] a) L. S. Lerman, *Proc. Natl. Acad. Sci. USA* **1971**, *68*, 1886–1890; b) V. V. Vasilevskaya, A. R. Khokhlov, Y. Matsuzawa, K. Yoshikawa, *J. Chem. Phys.* **1995**, *102*, 6595–6602.

[9] K. B. Roy, T. Antony, A. Saxena, H. B. Bohidar, *J. Phys. Chem. B* **1999**, *103*, 5117–5121.

[10] S. M. Mel'nikov, M. O. Khan, B. Lindman, B. Jonsson, *J. Am. Chem. Soc.* **1999**, *121*, 1130–1136.

[11] L. Cinque, Y. Ghomchi, Y. Chen, A. Bensimon, D. Baigl, *ChemBioChem* **2010**, *11*, 340–343.

[12] R. S. Dias, B. Lindman, M. G. Miguel, *J. Phys. Chem. B* **2002**, *106*, 12608–12612.

[13] A. González-Pérez, R. S. Dias, *Front. Biosci.* **2009**, *E1*, 228–241.

[14] a) A.-L. M. Le Ny, C. T. Lee, Jr., *J. Am. Chem. Soc.* **2006**, *128*, 6400–6408; b) M. Sollogoub, S. Guieu, M. Geoffroy, A. Yamada, A. Estévez-Torres, K. Yoshikawa, D. Baigl, *ChemBioChem* **2008**, *9*, 1201–1206.

[15] A. Estévez-Torres, C. Crozatier, A. Diguet, T. Hara, H. Saito, K. Yoshikawa, D. Baigl, *Proc. Natl. Acad. Sci. USA* **2009**, *106*, 12219–12223.

[16] Y.-C. Liu, A.-L. M. Le Ny, J. Schmidt, Y. Talmon, B. F. Chmelka, C. T. Lee, Jr., *Langmuir* **2009**, *25*, 5713–5724.

[17] A. Diguet, R.-M. Guillermic, N. Magome, A. Saint-Jalmes, Y. Chen, K. Yoshikawa, D. Baigl, *Angew. Chem.* **2009**, *121*, 9445–9448; *Angew. Chem. Int. Ed.* **2009**, *48*, 9281–9284.

[18] M. Geoffroy, D. Faure, R. Oda, D. M. Bassani, D. Baigl, *ChemBioChem* **2008**, *9*, 2382–2385.

[19] T. Hayashita, T. Kurosawa, T. Miyata, K. Tanaka, M. Igawa, *Colloid Polym. Sci.* **1994**, *272*, 1611–1619.

[20] K. Yoshikawa, Y. Matsuzawa, *Phys. D* **1995**, *84*, 220–227.

[21] K. Hayakawa, J. P. Santerre, J. C. T. Kwak, *Biophys. Chem.* **1983**, *17*, 175–181.

[22] R. Dias, S. Mel'nikov, B. Lindman, M. G. Miguel, *Langmuir* **2000**, *16*, 9577–9583.

[23] X. Liu, N. L. Abbott, *J. Colloid Interface Sci.* **2009**, *339*, 1–18.

[24] J. Eastoe, A. Vesperinas, *Soft Matter* **2005**, *1*, 338–347.

[25] C. T. Lee, Jr., K. A. Smith, T. A. Hatton, *Biochemistry* **2005**, *44*, 524–536.

[26] J. Eastoe, M. Sanchez Dominguez, P. Wyatt, R. K. Heenan, *Chem. Commun.* **2004**, 2608–2609.